Two-state one-dimensional spinless Fermi gas

J. K. Freericks and L. M. Falicov

Department of Physics, University of California—Berkeley, Berkeley, California 94720
and Materials and Chemical Sciences Division, Lawrence Berkeley Laboratory, Berkeley, California 94720
(Received 24 July 1989)

The two-state, one-dimensional, spinless Fermi gas (Falicov-Kimball model) is studied exactly by numerical calculation and perturbation theory. Rigorous results are presented for small interaction strength and (restricted) coherent and incoherent phase diagrams are calculated for two specific examples. The numerical calculations are extrapolated to provide a qualitative picture of the complete solution. The result includes a fractal structure in which the ground-state changes discontinuously as a function of the parameters.

I. INTRODUCTION

It is generally accepted that many properties of heavy-fermion systems and intermediate-valence compounds as well as the phenomena of metal-insulator transitions, itinerant magnetism, metallic crystallization, alloy formation, etc., result from the properties of strongly correlated electrons. There are, however, very few exact results available for correlated electronic systems, and approximate methods are sometimes contradictory. In 1969, the Falicov-Kimball model[1] was introduced as a model for metal-insulator transitions. It remains one of the simplest interacting fermion systems in which electron correlation effects may be studied exactly. Several rigorous results have already been obtained for the one-band spinless version of the Falicov-Kimball model: Brandt and Schmidt[2] calculated upper and lower bounds for the ground-state energy in two dimensions; Kennedy and Lieb[3] proved theorems on long-range order for arbitrary dimensions; Brandt and Mielsch[4] obtained an exact solution in infinite dimensions; and Jędrzejewski et al.[5] performed numerical studies in two dimensions. In this contribution we present additional rigorous results and restricted phase diagrams for the one-dimensional Falicov-Kimball model at $T = 0$.

The Hamiltonian for the one-dimensional Falicov-Kimball model defined on a lattice of N sites with periodic boundary conditions (PBC) is

$$H = -t \sum_{j=1}^{N} (c_j^{\dagger} c_{j+1} + c_{j+1}^{\dagger} c_j) + U \sum_{j=1}^{N} c_j^{\dagger} c_j W_j , \qquad (1)$$

where $c_j^{\dagger}$ (c_j) are fermionic creation (annihilation) operators for a spinless[6] electron at site j, W_j is a classical variable that is 1 (0) if an ion occupies (does not occupy) the jth site of the lattice, t is the hopping integral between nearest neighbors, and U is the ion-electron on-site interaction. The first term in (1) is the kinetic energy of the itinerant electrons and the second term is the interaction between electrons and ions. The total electron number $N_e = \sum_{j=1}^{N} c_j^{\dagger} c_j$ and the total ion number $N_i = \sum_{j=1}^{N} W_j$ are both conserved quantities.

The Hamiltonian (1) for the Falicov-Kimball model

has various physical interpretations. It was originally introduced to examine the mutual interaction of mobile d electrons (our electrons) with localized f electrons (our ions) in transition-metal oxides.[1] It has recently been proposed as a model for crystalline formation[3]—if the ion configuration $\{W_j\}$ of the ground state is periodic, then this model provides a mechanism for electron-induced crystalline order. It also describes a one-dimensional binary-alloy problem with the following map: occupied site yields ion of type A, empty site yields ion of type B, and $U \to U_A - U_B$ the difference in electron-ion site energy between ions of type A and type B. We finally note that the Hamiltonian (1) is identical to the one-dimensional tight-binding Schrödinger equation with an on-site potential that can assume two different values (0 and U). The tight-binding Schrödinger equation has been studied for random $\{W_j\}$ by mathematicians and physicists[7] and has been investigated recently for aperiodic deterministic sequences.[8]

Since the electrons do not interact among themselves, the energy levels of (1) are determined by the eigenvalues of H and the ground-state energy of a particular ion configuration $\Gamma \equiv \{W_j\}$ is found by filling in the lowest N_e one-electron levels. We let $E^{\Gamma}(X, N_e)$ denote the ground-state energy for N_e electrons in the ion configuration Γ with $X \equiv U/t$ (the hopping integral t determines the energy scale; all energies are measured in units of t). Many-body effects enter into the problem by considering the ground state for N_i ions

$$E(X, N_e, N_i) \equiv \min \left\{ E^{\Gamma}(X, N_e) \,\Big|\, N_i = \sum_{j=1}^{N} W_j \right\}, \qquad (2)$$

determined by comparing the $[N!/N_i!(N - N_i)!]$ ion configurations with fixed ion number. The minimization procedure in (2) determines the equivalence class of the ground-state ion configuration as a function of the interaction strength, the number of electrons, and the number of ions.

The Hamiltonian exhibits two kinds of particle-hole symmetries[3]—an ion-occupied–empty-site symmetry and an electron-hole symmetry. In the first case, we con-

sider the conjugate ion configuration Γ^* defined by interchanging occupied and unoccupied sites in the configuration Γ (this corresponds to $W_j^* = 1 - W_j$). The ground states for these two configurations are related:

$$E^{\Gamma^*}(X, N_e) = E^{\Gamma}(-X, N_e) + X N_e , \tag{3}$$

for all X and N_e. In the second case, we use the unitary transformation $c_j \rightarrow (-1)^j c_j$ and $c_j^\dagger \rightarrow (-1)^j c_j^\dagger$ to relate electron eigenvalues with interaction X to corresponding hole eigenvalues with interaction $(-X)$ yielding the result

$$E^{\Gamma}(X, N_e) = E^{\Gamma}(-X, N - N_e) + X N_i . \tag{4}$$

These two symmetries are used to reduce the necessary parameter space in the calculation of the $T = 0$ phase diagrams.

In the thermodynamic limit the number of lattice sites becomes infinite $(N \rightarrow \infty)$ but the electron $\rho_e \equiv N_e / N$ and the ion $\rho_i \equiv N_i / N$ concentrations remain finite. The ground-state energy per lattice site is determined from $n^{\Gamma}(E)$ the density of states (DOS)

$$E^{\Gamma}(X, \rho_e) = \int_{-\infty}^{E_F} n^{\Gamma}(E) E \, dE , \tag{5}$$

where E_F is the Fermi level and

$$\rho_e = \int_{-\infty}^{E_F} n^{\Gamma}(E) dE \tag{6}$$

for each ion configuration Γ. The DOS is calculated from the Green's function by

$$n(E) \equiv -\frac{1}{\pi} \text{Im} \lim_{\epsilon \rightarrow 0} G(E + i\epsilon) , \tag{7a}$$

$$G(E) \equiv \frac{1}{N} \sum_{j=1}^{N} G_j(E) , \tag{7b}$$

where the local Green's function is defined by the matrix element

$$G_j(E) \equiv \langle j | 1 / (E - H) | j \rangle .$$

A renormalized perturbation expansion[9] is used to determine the local Green's function exactly. The result,[9]

$$G_j(E) = \frac{1}{E - X W_j - \Delta_j^+(E) - \Delta_j^-(E)} , \tag{8}$$

is expressed in terms of continued fractions

$$\Delta_j^{\pm}(E) = \cfrac{1}{E - X W_{j\pm 1} - \cfrac{1}{E - X W_{j\pm 2} - \cfrac{1}{E - X W_{j\pm 3} - \cdots}}} , \tag{9}$$

where the local self-energy is $\Delta_j(E) = \Delta_j^+(E) + \Delta_j^-(E)$.

The continued fractions in (9) are evaluated straightforwardly for any periodic configuration Γ, since the variables W_j are then periodic and the fraction may be made finite. For example, the period-two case is analyzed by

$$\Delta_0^{\pm}(E) = \cfrac{1}{E - X W_1 - \cfrac{1}{E - X W_0 - \Delta_0^{\pm}(E)}} , \tag{10}$$

which yields

$$\Delta_0^{\pm}(E) = \tfrac{1}{2}\{E - X W_0 \pm [(E - X W_0)^2 (E - X W_1)^2 - 4(E - X W_0)(E - X W_1)]^{1/2} / (E - X W_1)\} , \tag{11}$$

and, for the DOS

$$n(E) = \frac{1}{2\pi} \text{Re} \frac{|E - X W_0| + |E - X W_1|}{\{-(E - X W_0)(E - X W_1)[E^2 - X(W_0 + W_1)E + X^2 W_0 W_1 - 4]\}^{1/2}} . \tag{12}$$

In addition to the one-phase periodic configurations, we consider one physically relevant two-phase configuration called the segregated phase. The segregated phase is an incoherent mixture of the empty and full lattices with weights $(1 - \rho_i)$ and ρ_i, respectively. The segregated phase has the physical interpretation of the case where the ions clump together and do not form a periodic arrangement (crystallization model) or of the case where the ions of type A and the ions of type B are immiscible and separate (alloy model). The DOS is trivial for the segregated phase, since it is a weighted linear combination,

$$n^{\text{seg}}(E) = (1 - \rho_i) n^{\text{empty}}(E) + \rho_i n^{\text{full}}(E) , \tag{13}$$

of the DOS for the empty and full lattices.

The segregated phase is also important, since it is expected to be the ground state in the limit $|X| \rightarrow \infty$. In this limit the potential barrier is so large that the elec-trons are trapped between ion-occupied–empty-site boundaries. The dominant contribution to the ground-state energy is the kinetic energy of the electrons, which is minimized by making the box as large as possible. This favors the segregated phase to be the ground state. However, at the point where the electrons completely fill the box $(\rho_e = 1 - \rho_i$ for $X \rightarrow +\infty$ and $\rho_e = \rho_i$ for $X \rightarrow -\infty)$ the Pauli exclusion principle requires the additional electrons to be placed above a large potential barrier. At this point a periodic arrangement of the ions may actually lower the ground-state energy. These physical ideas are summarized in what we may call the *segregation principle*: In the limit $|X| \rightarrow \infty$ the segregated phase is the ground state for all values of the electron concentration except the specific values $\rho_e = 1 - \rho_i$ for $X \rightarrow +\infty$, and $\rho_e = \rho_i$ for $X \rightarrow -\infty$. We have found that *principle* to be true in all calculated cases, and we expect it to hold for all values of ρ_e and ρ_i.

In the following section we use perturbation theory to analyze the structure of the ground-state phase diagram near $X = 0$. In Secs. III and IV we examine in detail the cases with ionic densities of $\rho_i = \frac{1}{2}$ and $\rho_i = \frac{1}{3}$, respectively, and give complete phase diagrams for the segregated phase and all ionic configurations with periods less than 10 compatible with those ρ_i. We present our conclusions in the final section.

II. PERTURBATIVE ANALYSIS

In the limit $X \ll 1$ we can perform a perturbative analysis of the Hamiltonian (1) and determine the structure of the phase diagrams for small interaction strength.

We only consider periodic structures to avoid the technical difficulties associated with aperiodic configurations. Suppose the configuration $\Gamma(r)$ has period r; that is, $W_{j+r} = W_j$ for all j. The Fourier coefficient $W(2\pi n /r)$ is defined

$$W(2\pi n /r) \equiv \frac{1}{N} \sum_{j=1}^{N} e^{-i(2\pi nj/r)} W_j$$

$$= \frac{1}{r} \sum_{j=1}^{r} e^{-i(2\pi nj/r)} W_j \tag{14}$$

for $n = 0, 1, \ldots, r-1$. Straightforward Rayleigh-Schrödinger perturbation theory through second order, with the second term in (1) as the perturbation, yields the expression

$$E^{\Gamma(r)}(X,\rho_e) = -\frac{2}{\pi}\sin(\pi\rho_e) + X\rho_e\rho_i + \frac{X^2}{8\pi}\sum_{n=1}^{r-1}\frac{|W(2\pi n /r)|^2}{\sin(\pi n /r)}\ln\left|\frac{\sin(\pi n /r)-\sin(\pi\rho_e)}{\sin(\pi n /r)+\sin(\pi\rho_e)}\right| + O(X^3) \tag{15}$$

for the ground-state energy of configuration $\Gamma(r)$. The minimization procedure (2) already outlined considers configurations with the same ion concentration at fixed electron concentration and interaction strength, so that the ground-state energy is degenerate up to first order. The second-order term has a logarithmic singularity at $\rho_e = n/r$ with relative strength $|W(2\pi n /r)|^2$. The singularity indicates that perturbation theory fails at these critical electron concentrations; by comparing the strength of the singularity for different configurations, the ground state can be determined in the region near $\rho_e = n /r$ (and by continuity at $\rho_e = n /r$).

In fact, if we restrict the minimization in (2) to be only over *periodic* configurations, then for rational concentrations the ground-state configuration has the *lowest* allowed periodicity (this is expected from a Fermi-surface nesting argument: The state with the largest gap at the Fermi level is the ground state). More rigorously we prove the following theorem.

Theorem (1). Given rational electron and ion concentrations

$$\rho_e = \frac{p_e}{q_e}, \quad \rho_i = \frac{p_i}{q_i} , \tag{16}$$

with p_e relatively prime to q_e and p_i relatively prime to q_i, then the periodic configuration with the lowest energy has period $Q = \text{lcm}(q_e, q_i)$, where lcm stands for least common multiple. The proof is given in the Appendix and includes an expression for the ion configuration $\Gamma(Q)$ corresponding to the lowest-energy state.

These lowest-energy configurations satisfy certain structural properties. Let l denote the length of the largest connected island of occupied sites in the configuration $\Gamma(Q)$ [e.g., the configuration XXXOXOXXOO, where X represents an ion and O represents an empty site, corresponds to a given $\Gamma(10)$ and has $l = 3$], then a configuration in which only islands of length l and $(l-1)$ appear is defined to have the uni-

form ion distribution property. For example, XXOXXOOO has the uniform ion distribution property but XXXOOXOO does not. The uniform empty-site distribution property is analogously defined. This characterization of the ground-state configuration in the limit $X \to 0$ is summarized in the following theorem.

Theorem (2). In the limit $X \to 0$ any periodic lowest-energy configuration with $\rho_i \leq \frac{1}{2}$ has the uniform ion distribution property and any periodic lowest-energy configuration with $\rho_i \geq \frac{1}{2}$ has the uniform empty-site distribution property. The proof is given in the Appendix.

The ground-state energy of the segregated phase also has a perturbative expansion about $X = 0$. A straightforward analysis using the DOS in Eq. (13) yields

$$E^{\text{seg}}(X,\rho_e) = -\frac{2}{\pi}\sin(\pi\rho_e) + X\rho_e\rho_i$$

$$-\frac{X^2}{4\pi}\frac{\rho_i(1-\rho_i)}{\sin(\pi\rho_e)} + O(X^3) \tag{17}$$

for the ground-state energy of the segregated phase that is valid in the two-phase, band-overlap region

$$\delta(X) < \rho_e < 1 - \delta(X) ,$$

where

$$\delta(X) = \frac{\sqrt{|X|}}{\pi}[\Theta(-X)\rho_i + \Theta(X)(1-\rho_i)] , \tag{18}$$

and $\Theta(X)$ is the unit step function. This expansion has a singularity in the limit $X \to 0$ and $\rho_e \to 0$, which indicates that the segregated phase should be the ground state for low electron concentrations.

The solution for the ground-state configuration of the one-dimensional Falicov-Kimball model is conveniently summarized in a coherent phase diagram. The ion concentration is fixed at $\rho_i = p_i/q_i$ and the ground-state configuration is plotted as a function of the electron concentration and the interaction strength. We choose the

segregated phase as the zero of the energy scale because of its physical relevance. We limit ourselves to the case $\rho_i \leq \frac{1}{2}$ and $\rho_e \leq \frac{1}{2}$, since the other cases can be obtained by application of the symmetries (3) and (4). The two preceding theorems indicate that in the limit $X \to 0$ the coherent phase diagram has a discontinuous, fractal structure, with a different periodic ground-state configuration at each rational ρ_e. These configurations all satisfy the relevant uniform-distribution property and appear to be a regular transition from the segregated phase at $\rho_e \to 0$ to a period q_i ($2q_i$) state at $\rho_e = \frac{1}{2}$ if q_i is even (odd). The inclusion of aperiodic configurations is not expected to change this general picture. Recent analysis[8] indicates that some aperiodic configurations have gaps at rational numbers (where we expect the periodic configurations to be lower in energy) and at irrational numbers (where the aperiodic configurations may be lower in energy). Therefore, we conjecture that in the limit $X \to 0$ the ground-state configuration changes, point by point, at every value of ρ_e and the coherent phase diagram has a regular (discontinuous) transition pattern from the segregated phase at $\rho_e \to 0$ to a periodic phase at $\rho_e = \frac{1}{2}$. We also conjecture that the relevant uniform-distribution property holds for each of the ground-state configurations.

III. THE CASE $\rho_i = \frac{1}{2}$

In this section we examine in detail the half-full ion case and present our results in the form of phase diagrams. We restrict ourselves to the case $\rho_e \leq \frac{1}{2}$ by using the electron-hole symmetry (4); the phase diagram for the region $\rho_e \geq \frac{1}{2}$ is determined by rotating the region $\rho_e \leq \frac{1}{2}$ by 180° about the point $X = 0$, $\rho_e = \frac{1}{2}$. We further restrict ourselves to the case $X \geq 0$ by using the ion-occupied–empty-site symmetry (3); the phase diagram for the region $X \leq 0$ is determined by reflecting the region $X \geq 0$ in a mirror plane along the $X = 0$ axis and applying the conjugation operation to the ion configurations (each configuration Γ with $\rho_i = \frac{1}{2}$ is either self-conjugate $\Gamma^* = \Gamma$ or forms a conjugation pair with another $\rho_i = \frac{1}{2}$ configuration). We finally restrict ourselves to consider only the segregated phase, all periodic phases with $\rho_i = \frac{1}{2}$ and periods less than 9, and any incoherent mixture of
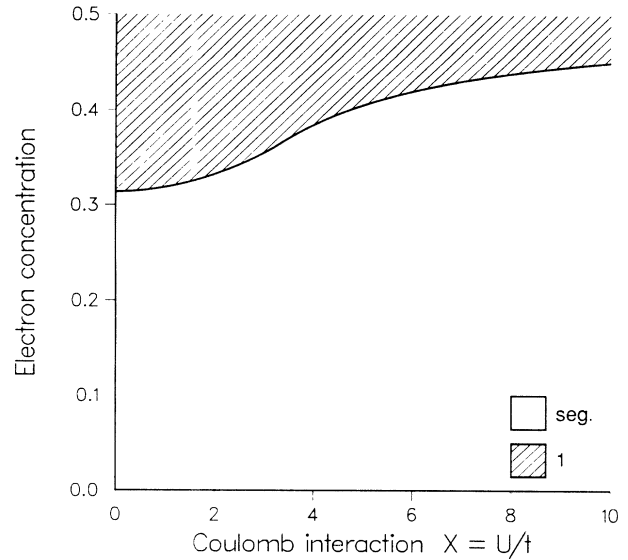

FIG. 1. Calculated coherent phase diagram for the segregated and period-two phases with $\rho_i = \frac{1}{2}$. See Table I for the key to the legend.

these phases. These periodic phases are summarized in Table I. The ground-state energies are calculated exactly using the Green's-function technique outlined in Sec. I.

The coherent phase diagrams are determined by comparing the energy of each periodic phase with energy of the segregated phase and plotting the lowest-energy state as a function of the electron concentration ρ_e and the interaction strength X. The results are presented in Figs. 1–4 and exhibit the extremely rich structure of the solutions of the mode. We summarize these results with some observations: (a) The periodic ground-state

TABLE I. Periodic configurations for the $\rho_i = \frac{1}{2}$ case.

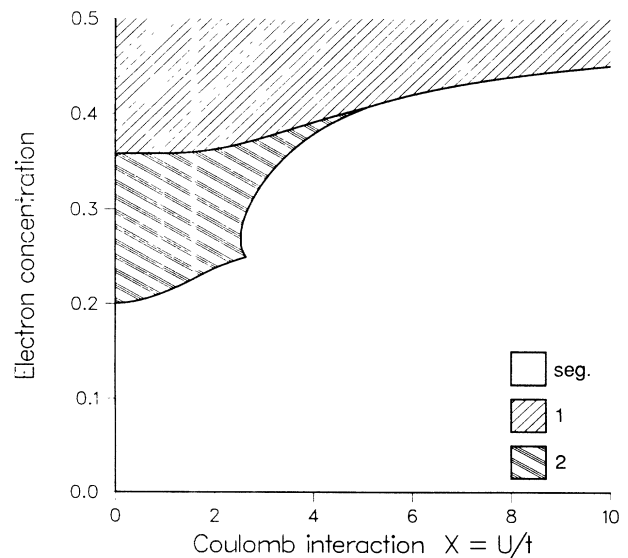|	Configuration	Conjugate
1	XO	1
2	XXOO	2
3	XXXOOO	3
4	XXOXOO	4
5	XXXXOOOO	5
6	XXXOXOOO	6
7	XXXOOXOO	8
8	XXOXXOOO	7
9	XXOXOXOO	9
10	XXOXOOXO	10

FIG. 2. Calculated coherent phase diagram for the segregated, period-two and period-four phases with $\rho_i = \frac{1}{2}$. See Table I for the key to the legend.
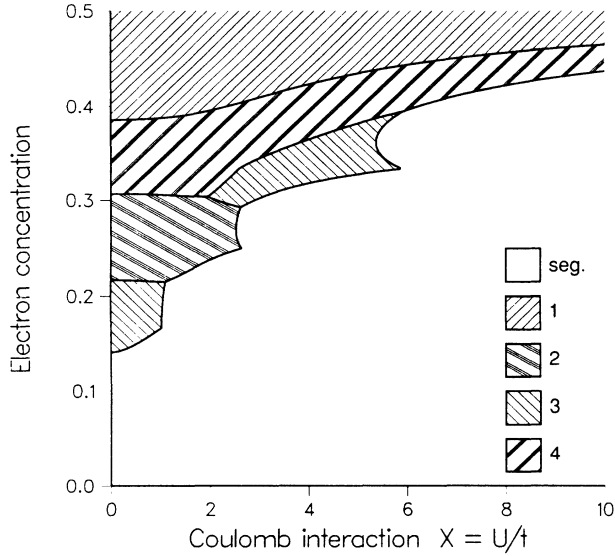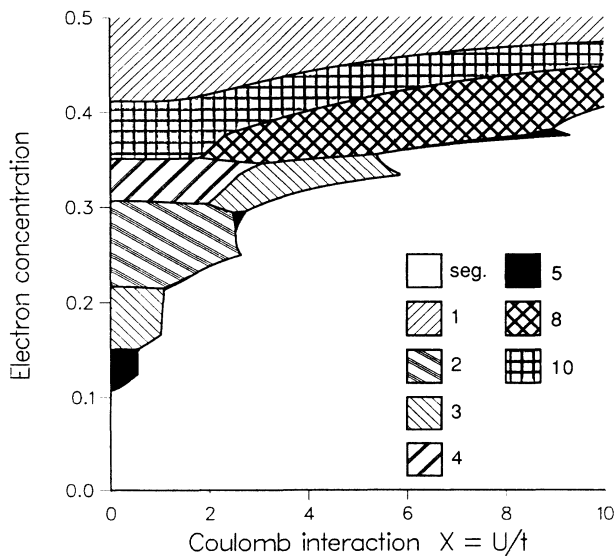
FIG. 3. Calculated coherent phase diagram for the segregated, period-two, period-four, and period-six phases with $\rho_i = \frac{1}{2}$. See Table I for the key to the legend.

theorem and both uniform-distribution properties hold in the region $|X| \ll 1$. (b) The alternating phase XO is the ground state at $\rho_e = \frac{1}{2}$ for all values of X as stated by previous investigations.[2,3] (c) The phase diagrams tend to simplify as the interaction strength increases indicating that many-body effects stabilize the system (this is a consequence of the segregation principle). (d) There is a trend for phases that disappear from the phase diagram as X increases to reappear as phase islands at even larger values of X (e.g., the XXXOOO phase in Figs. 3 and 4 and the XXXXOOOO phase in Fig. 4). (e) Phase islands

of configurations not present at $X = 0$ may form at larger values of X (e.g., the XXOXXOOO phase in Fig. 4). (f) The uniform-distribution properties may not hold at finite values of X. (The XXOXXOOO phase in Fig. 4 does not satisfy the uniform empty-site distribution property and its conjugate does not satisfy the uniform ion distribution property.) (g) Some configurations are not the ground state for any value of X or ρ_e (e.g., the configurations XXXOXOOO and XXOXOXOO do not appear in Fig. 4).

The incoherent phase diagrams are determined by choosing the minimal energy state, allowing for incoherent mixing[10] of the $\rho_i = \frac{1}{2}$ periodic phases with themselves and with the segregated phase (which is already an incoherent mixture of the $\rho_i = 0$ and $\rho_i = 1$ phases). This is accomplished by constructing the convex hull of the ground-state energy curves for fixed X and assigning an incoherent phase mixture to each region where the convex hull is lower than the energy curves. The results are presented in Figs. 5–8 where solid lines and shaded regions correspond to single phases, dashed lines correspond to two-phase mixtures and dotted lines correspond to more than two-phase mixtures (the points where vertical dotted lines pass through horizontal solid lines are the points of phase transitions.) The numbers above the single-phase lines identify the ground state according to the numbers in Table I. The unshaded region below the dashed line is the region where the segregated phase is the ground state. The unshaded regions between a solid (or dashed) line and a solid line are the regions where an incoherent mixture of the two (or three) phases is the ground state. We make the following observations: (h) The incoherent phase diagrams are simpler than their single-phase counterparts. The regions enclosing finite areas of single phases are drastically reduced. (i) The be-

FIG. 4. Calculated coherent phase diagram for the segregated, period-two, period-four, period-six, and period-eight phases with $\rho_i = \frac{1}{2}$. See Table I for the key to the legend.
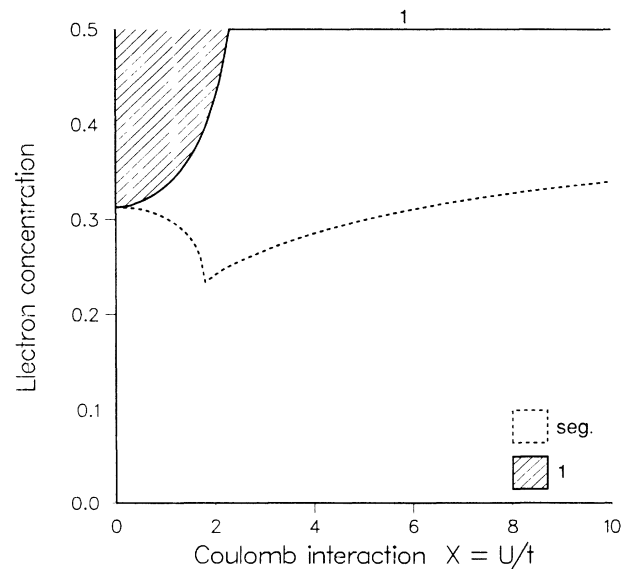

FIG. 5. Calculated incoherent phase diagram for the segregated and period-two phases with $\rho_i = \frac{1}{2}$. See Table I for the key to the legend.
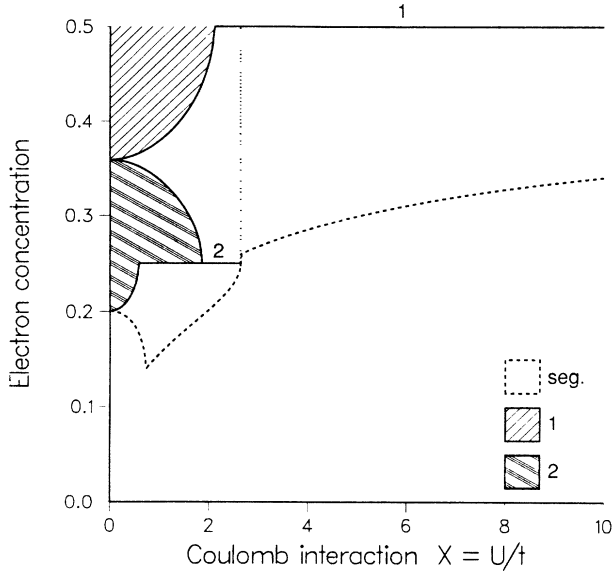
FIG. 6. Calculated incoherent phase diagram for the segregated, period-two and period-four phases with $\rho_i = \frac{1}{2}$. See Table I for the key to the legend.
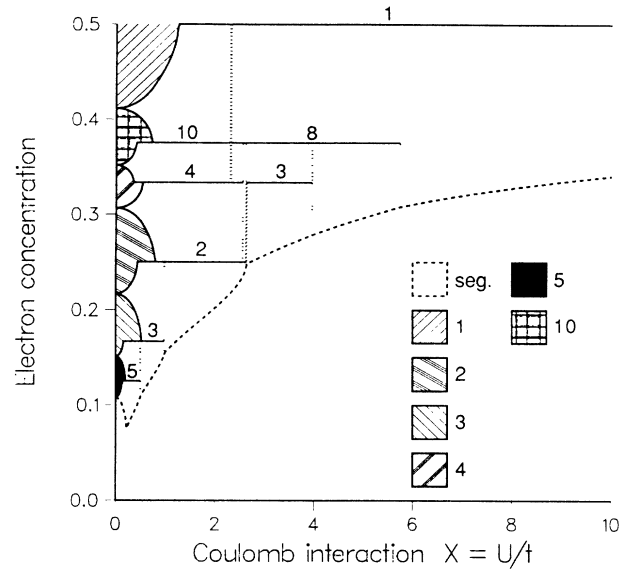

FIG. 8. Calculated incoherent phase diagram for the segregated, period-two, period-four, period-six, and period-eight phases with $\rho_i = \frac{1}{2}$. See Table I for the key to the legend.

havior in the limit $|X| \to 0$ appears to be the same as that predicted by perturbation theory for the coherent diagrams. (j) The secondary phase islands that sometimes form at $|X| > 0$ either become single phase lines (XXXOOO in Figs. 7 and 8) or vanish altogether (XXXXOOOO in Fig. 8).

These incoherent phase diagrams are important to study for two reasons: First, they determine the ground state of a real system, since any physical system organizes itself in an incoherent mixture of phases to minimize en-
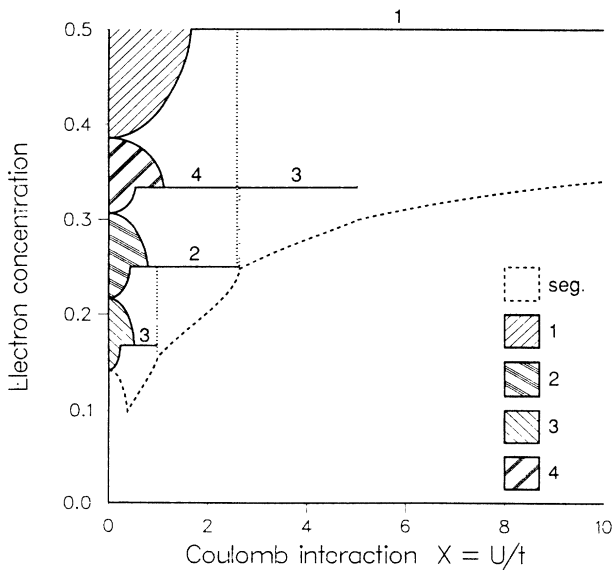

FIG. 7. Calculated incoherent phase diagram for the segregated, period-two, period-four, and period-six phases with $\rho_i = \frac{1}{2}$. See Table I for the key to the legend.

ergy (if possible); second, they produce a better approximation to the complete phase diagram of the Falicov-Kimball model. This is because any incoherent mixture of phases can be reinterpreted as an aperiodic configuration in a coherent phase diagram. By using this reinterpretation we strengthen the perturbation theory results of Sec. II to conjecture that the ground-state configuration is the segregated phase for a finite region $[0 \leq \rho_e < \rho_e^{max}(X)]$; above this region the ground-state configuration changes point by point with ρ_e, and has a regular (discontinuous) transition from the segregated phase to a periodic phase at $\rho_e = \frac{1}{2}$. Furthermore, for the case $\rho_i = \frac{1}{2}$ we must have $\rho_e^{max}(X) < \frac{1}{2}$, since the alternating state XO is the ground state[2,3] at $\rho_e = \frac{1}{2}$ for all X.

IV. THE CASE $\rho_i = \frac{1}{3}$

We examine the one-third-full ion case as a representative of the general case because it does not have any extra symmetries. The electron-hole symmetry (4) allows us to consider only the case $\rho_e \leq \frac{1}{2}$, but we must consider all values of X, since the ion-occupied–empty-site symmetry (3) produces the phase diagrams for the $\rho_i = \frac{2}{3}$ case. We consider only the segregated phase, the period-three, period-six, and period-nine phases with $\rho_i = \frac{1}{3}$, and any incoherent mixture of these phases.[10] The precise ion configurations considered are summarized in Table II.

The results for the coherent phase diagrams are presented in Figs. 9–11 and they exhibit a marked asymmetry with respect to the $X = 0$ plane. We make the following observations: (k) There is no evidence in support of or against the uniform ion distribution property, since this property can only be observed for period-12 phases and larger, which are not studied here. (l) The periodic ground-state theorem holds for $|X| \ll 1$, but the many-

TABLE II. Periodic configurations for the $\rho_i = \frac{1}{3}$ case.

	Configuration
1	XOO
2	XXOOOO
3	XOXOOO
4	XXXOOOOOO
5	XXOXOOOOO
6	XXOOXOOOO
7	XXOOOXOOO
8	XOXOXOOOO
9	XOXOOXOOO

body effects rapidly become more important and change the structure of the phase diagrams. (m) It appears that the period-three phase XOO is the ground state at $\rho_e = \frac{1}{3}$ for all values of X less than zero. (n) The segregation principle holds; in the limit $|X| \to -\infty$ the segregated phase is the ground state for all values of ρ_e except for a region about $\rho_e = \frac{1}{3}$ and $X \to -\infty$. (o) There is still a trend for phases present at $X = 0$ to appear as phase islands at larger values of $|X|$ (e.g., the XXOOOO phase in Figs. 10 and 11, the XOXOOO phase in Fig. 10, the XXXOOOOOO phase in Fig. 11, and the XXOOOXOOO phase in Fig. 11). (p) All studied configurations are the ground state for some value of the parameters ρ_e and X.

The results for the incoherent phase diagrams are summarized in Figs. 12–14. We present the following observations: (q) Observations (h), (i), and (j) of Sec. III still hold. (r) Two phases (XXOOXOOO and XOXOOXOOO) do not appear in the incoherent phase diagram although they were present in the coherent phase diagram.

FIG. 10. Calculated coherent phase diagram for the segregated, period-three, and period-six phases with $\rho_i = \frac{1}{3}$. See Table II for the key to the legend.

The structure for the full Falicov-Kimball model in the general case emerges from these incoherent phase diagrams. If we reinterpret an incoherent mixture of phases as an aperiodic phase in the coherent phase diagram, then it appears that at each value of X there is a finite region where the segregated phase is the ground state. In the rest of the region the ground state changes from point to point with ρ_e and has a regular (discontinuous) transition from the segregated phase to a periodic phase and (possibly) back to the segregated phase.
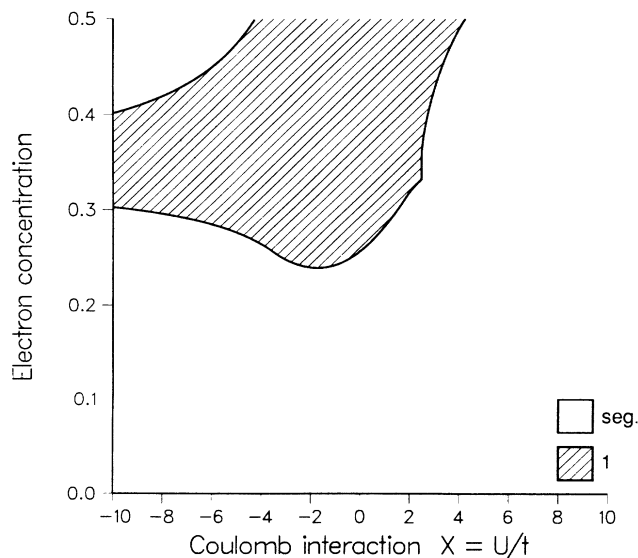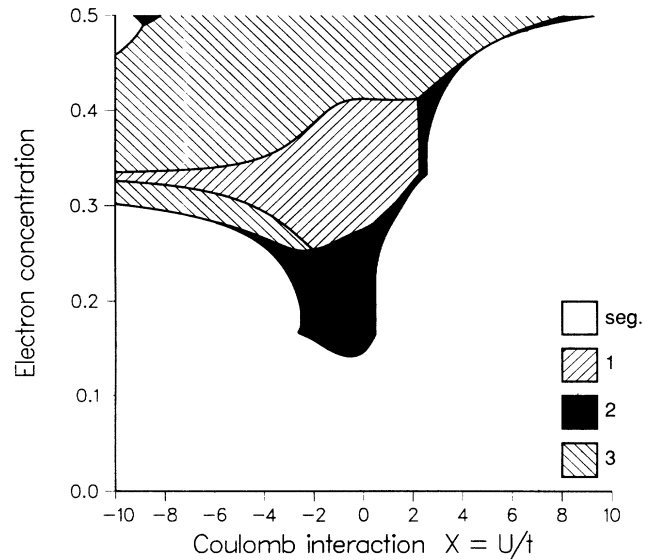

FIG. 9. Calculated coherent phase diagram for the segregated and period-three phases with $\rho_i = \frac{1}{3}$. See Table II for the key to the legend.
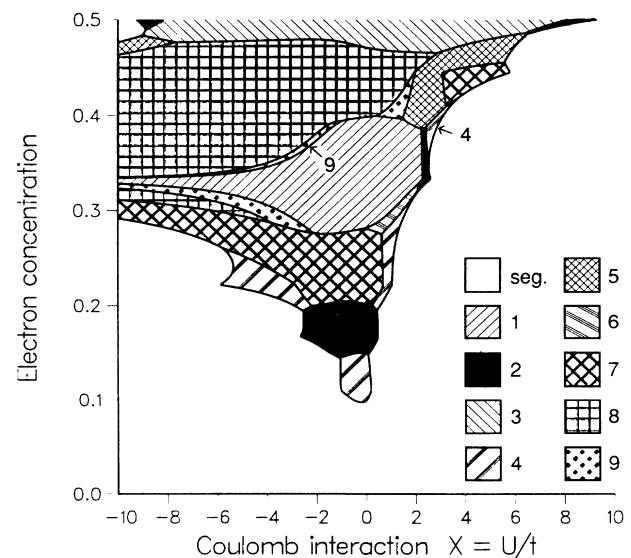

FIG. 11. Calculated coherent phase diagram for the segregated, period-three, period-six, and period-nine phases with $\rho_i = \frac{1}{3}$. See Table II for the key to the legend.
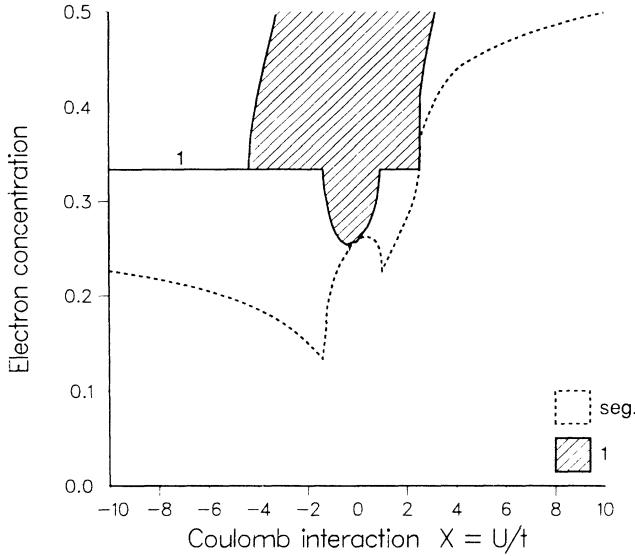
FIG. 12. Calculated incoherent phase diagram for the segregated and period-three phases with $\rho_i = \frac{1}{3}$. See Table II for the key to the legend.

FIG. 14. Calculated incoherent phase diagram for the segregated, period-three, period-six, and period-nine phases with $\rho_i = \frac{1}{3}$. See Table II for the key to the legend.

V. CONCLUSION

Since its introduction 20 years ago, the Falicov-Kimball model[1] is one of the simplest models of interacting electron systems. We have studied the one-dimensional version of this model by exact numerical calculation for a restricted number of phases and by perturbation theory for small interaction strength. Our rigorous results include a periodic ground-state theorem and uniform ion and empty-site distribution properties

for rational electron and ion concentrations and small interaction strength. Our numerical calculations indicate that the phase diagram of the complete model is separated into two distinct regions: In the first region the segregated phase is the ground state, and in the second region the phase diagram has a complex structure with the ground state apparently changing point by point at every value of the electron concentration for fixed interaction strength. In this second region the ground state has a regular (discontinuous) transition pattern from the segregated phase to a periodic phase and back to the segregated phase.

We also present two unproven conjectures that characterize further the structure of the phase diagram as illustrated by our numerical work. The first is called the segregation principle, which states at large interaction strength that the segregated phase is the ground state for almost all electron concentrations. The only exceptions are when the electron concentration matches the ion or the empty-site concentration, where a periodic phase is the ground state. The second is the uniform ion or empty-site distribution property, which states that the ground-state configurations satisfy certain structural characteristics. The properties are true for small interaction strength but appear to be violated for moderate interactions.

We mention one final open question. The proper incoherent phase diagram is plotted as a function of the electron and ion concentrations. We have evaluated the restricted phase diagrams for only five ion concentrations ($\rho_i = 0, \frac{1}{3}, \frac{1}{2}, \frac{2}{3}, 1$) and have no concrete conjecture for the structure of the incoherent phase diagram. However, we expect this phase diagram to separate into two regions with simple behavior in one region and complex behavior in the other.
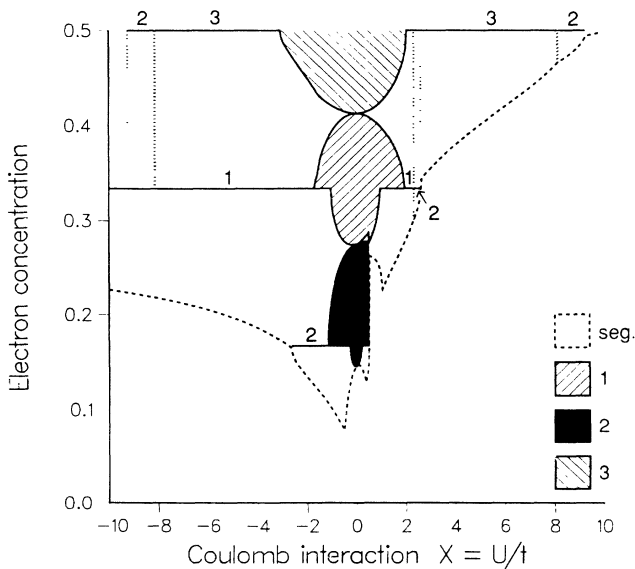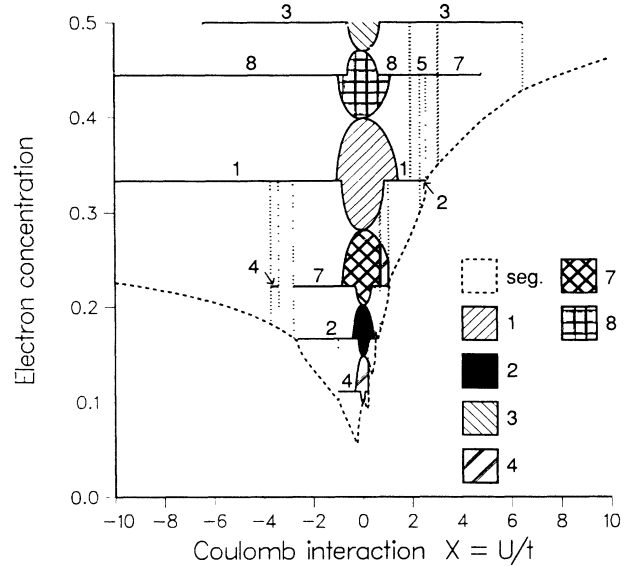

FIG. 13. Calculated incoherent phase diagram for the segregated, period-three and period-six phases with $\rho_i = \frac{1}{3}$. See Table II for the key to the legend.

ACKNOWLEDGEMENTS

APPENDIX: PROOF OF THE PERIODIC GROUND-STATE THEOREMS

In this appendix we prove the two theorems stated in Sec. II. We begin with the periodic ground-state theorem.

Theorem (1). Given rational electron and ion concentrations

$$\rho_e = \frac{p_e}{q_e}, \quad \rho_i = \frac{p_i}{q_i}, \tag{A1}$$

with p_e relatively prime to q_e and p_i relatively prime to q_i, then the periodic configuration with the lowest energy has period $Q = \text{lcm}(q_e, q_i)$.

Proof. The periodic configuration with the lowest energy is the configuration with the largest square Fourier coefficient $|W(2\pi\rho_e)|^2$. The trial configurations that have nonzero Fourier coefficient and proper ion concentration must have a periodicity that is a multiple of Q. Consider all periodic configurations with ion concentration ρ_i and with period less than or equal to $r = mQ$. These configurations all lie on a lattice with PBC and size $N = MQ$, where $M = \text{lcm}(1, 2, \ldots, m)$. We show the configuration with the lowest energy in this restricted set has period Q which (since m is arbitrary) proves the theorem.

The proof proceeds by construction of the largest $|W(2\pi\rho_e)|^2$. Assume, for simplicity, that $q_e = Q$. Define integers k_i by the relation

$$(p_e k_i)\text{mod}Q = i, \quad i = 0, 1, \ldots, Q - 1. \tag{A2}$$

Then the choice of $W_j = 1$ for

$$j = k_i + lQ, \quad i = 0, 1, \ldots, Qp_i/q_i - 1,$$
$$l = 0, 1, \ldots, M - 1 \tag{A3}$$

gives an ion concentration

$$\rho_i = \frac{1}{N} \sum_{j=0}^{N-1} W_j = \frac{p_i}{q_i}, \tag{A4}$$

and maximizes the square Fourier coefficient

$$|W(2\pi\rho_e)|^2 = \frac{1}{N^2} \sum_{j,k} W_j W_k \cos[2\pi p_e(j-k)/Q] \tag{A5a}$$

$$= \frac{1}{Q^2} \left[Qp_i + 2 \sum_{j=1}^{Qp_i/q_i - 1} (Qp_i/q_i - j) \right.$$

$$\left. \times \cos(2\pi j/Q) \right], \tag{A5b}$$

since the summation in (A5a) has the maximal allowed number of $(j-k)\text{mod}Q = 0$, $(j-k)\text{mod}Q = 1, \ldots$, and $(j-k)\text{mod}Q = Qp_i/q_i - 1$. The preceding minimal configuration $\Gamma(Q)$ constructed has period Q, which completes the proof. The proof for the case $q_e \neq Q$ is similar and is omitted here. The only complication of this case is that the second-order perturbation theory may not fully lift the degeneracy of the lowest-energy state. These degenerate states all have period Q, however, which is sufficient to prove the theorem.[11]

As an example, we consider the case $\rho_e = \frac{3}{8}$ and $\rho_i = \frac{1}{2}$. This gives $Q = 8$ with $k_0 = 0$, $k_1 = 3$, $k_2 = 6$, and $k_3 = 1$, so that the configuration XXOXOOXO is the lowest-energy periodic state in the limit $X \to 0$.

We continue with the proof of the uniform-distribution properties.

Theorem (2). In the limit $X \to 0$ any periodic lowest-energy configuration with $\rho_i \leq \frac{1}{2}$ has the uniform ion distribution property and any periodic lowest-energy configuration with $\rho_i \geq \frac{1}{2}$ has the uniform empty-site distribution property.

Proof. We restrict ourselves to the case $\rho_i \leq \frac{1}{2}$ and $\rho_e \leq \frac{1}{2}$, since the other cases immediately follow upon application of the symmetries (3) and (4). Assume that $q_e = Q$ (the proof of the more general case is similar and is omitted). The Q integers $\{k_i\}$ can be represented in terms of the first p_e integers by

$$k_{sp_e + j} = k_j + s, \quad j = 0, 1, \ldots, p_e - 1, \quad s = 0, 1, \ldots, r - 1, \tag{A6}$$

and

$$k_{rp_e + j} = k_j + r, \quad j = 0, 1, \ldots, t - 1, \tag{A7}$$

where $Q = rp_e + t$ and $t < p_e$. Since each integer from 0 to $Q - 1$ appears in $\{k_i\}$ once and only once, the nearest neighbors in the first p_e integers $k_0, k_1, \ldots, k_{p_e - 1}$ are separated by gaps of length r or $r - 1$ (there are t neighbors with separation r and $p_e - t$ neighbors with separation $r - 1$). As the ions are filled in according to the prescription (A3) of theorem (1), each configuration will satisfy the uniform ion distribution property until the gap between any two nearest neighbors in the original p_e ions is filled in. This occurs when $\rho_i > 1 - \rho_e$, which is not possible by the hypothesis and proves the theorem.

[1]L. M. Falicov and J. C. Kimball, Phys. Rev. Lett. **22**, 997 (1969).

[2]U. Brandt and R. Schmidt, Z. Phys. B **63**, 45 (1986); **67**, 43 (1987).

[3]T. Kennedy and E. H. Lieb, Physica **138A**, 320 (1986); E. H. Lieb, *ibid.* **140A**, 240 (1986).

[4]U. Brandt and C. Mielsch, Z. Phys. B **75**, 365 (1989).

[5]J. Jędrzejewski, J. Lach, and R. Łyżwa, Phys. Lett. A **134**, 319 (1989); Physica **154A**, 529 (1989).

[6]Spin may be introduced by simply doubling the allowed electron occupancy of each lattice site, since the electrons do not interact with themselves in this model.

[7]B. Simon, Adv. Appl. Math. **3**, 463 (1982); E. N. Economou, C. M. Soukoulis, and M. H. Cohen, Phys. Rev. B **37**, 4399 (1988).

[8]K. Machida and M. Nakano, Phys. Rev. B **34**, 5073 (1986); Z. Cheng, R. Savit and R. Martig, *ibid.* **37**, 4375 (1988); J. M. Luck, *ibid.* **39**, 5834 (1989); D. Würtz, T. Schneider, A. Politi, and M. Zanneti, *ibid.* **39**, 7829 (1989).

[9]P. W. Anderson, Phys. Rev. **109**, 1492 (1958); E. N. Economou and M. H. Cohen, Phys. Rev. B **4**, 396 (1971); E. N. Economou, *Green's Functions in Quantum Physics*, 2nd ed. (Springer-Verlag, Heidelberg, 1983).

[10]In theory, one can mix configurations with any ion concentrations as long as the mixed phase has the proper ion and electron average concentrations. We are forming only the simplest mixtures.

[11]Higher-order perturbation theory may lift any residual degeneracy of this case.